Electronic Supplementary Material (ESI) for Materials Horizons.
This journal is © The Royal Society of Chemistry 2024

Supporting Information

An Ultra-Soft Conductive Elastomer for Multifunctional Tactile Sensors with High Range and Sensitivity.

Ao Yin[ab], Ruiguang Chen[ab], Rui Yin[ab], Shiqiang Zhou[ab], Yang Ye[ab], Yuxin Wang[ab], Peike Wang[ab], Xue Qi[ab], Haipeng Liu[ab], Jiang Liu[ab], Suzhu Yu[ab]* and Jun Wei[abc]*

[a]*Shenzhen Key Laboratory of Flexible Printed Electronics Technology, Harbin Institute of Technology (Shenzhen), Shenzhen 518055, China*

[b]*School of Materials Science and Engineering, Harbin Institute of Technology (Shenzhen), Shenzhen 518055, China*

[c]*State Key Laboratory of Advanced Welding and Joining, Harbin Institute of Technology, Harbin 150001, China*

*Corresponding author: Suzhu Yu, Jun Wei, ***E-mail***: szyu@hit.edu.cn, junwei@hit.edu.cn

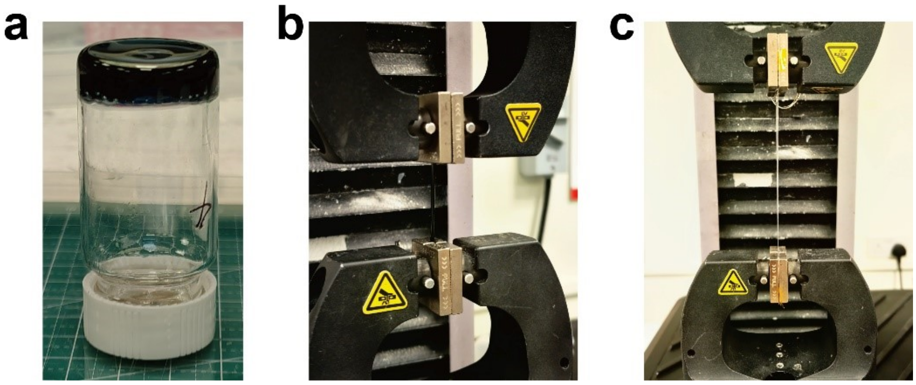

Figure S1. (a) Blended solution with 18% content PVA after 15 min. The photo of the tensile test using MST-42 of (b) PM2 and (c) the dielectric layer.

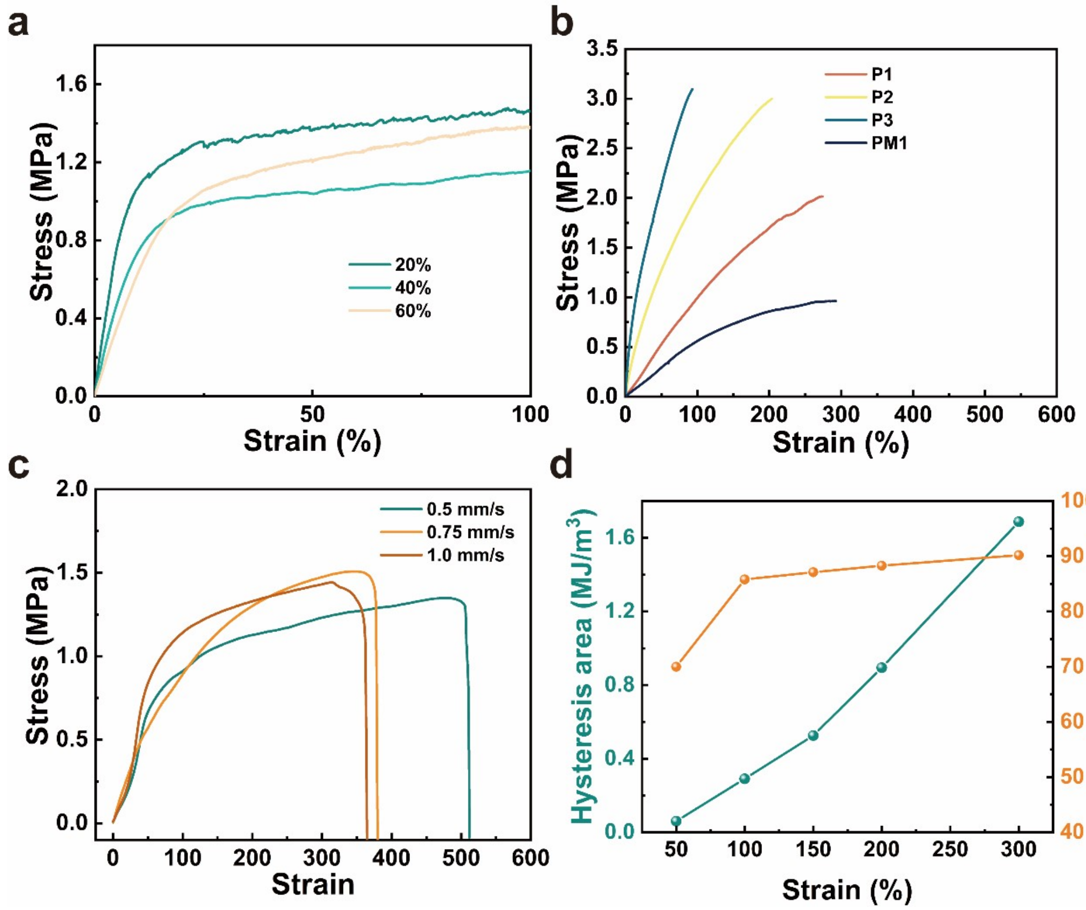

Figure S2. Stress-strain curves of (a) dielectric layer with different content of ILs and (b) SCCFs with different content of PEDOT:PSS and (c) PM2 sample under different deformation rates. (d) Plot of hysteresis area and hysteresis ratio versus strain of PM2 in the strain range from 50% to 300% at a deformation rate of 0.2 mm/s.

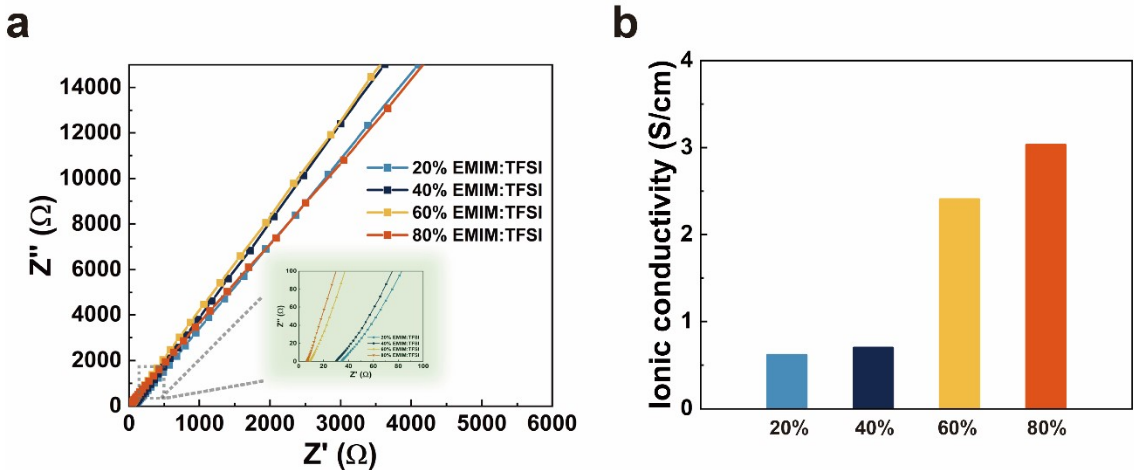

Figure S3. (a) AC impedance spectra of the dielectric layer with different IL content. (b) The calculated conductivity of the dielectric layer with different IL content.

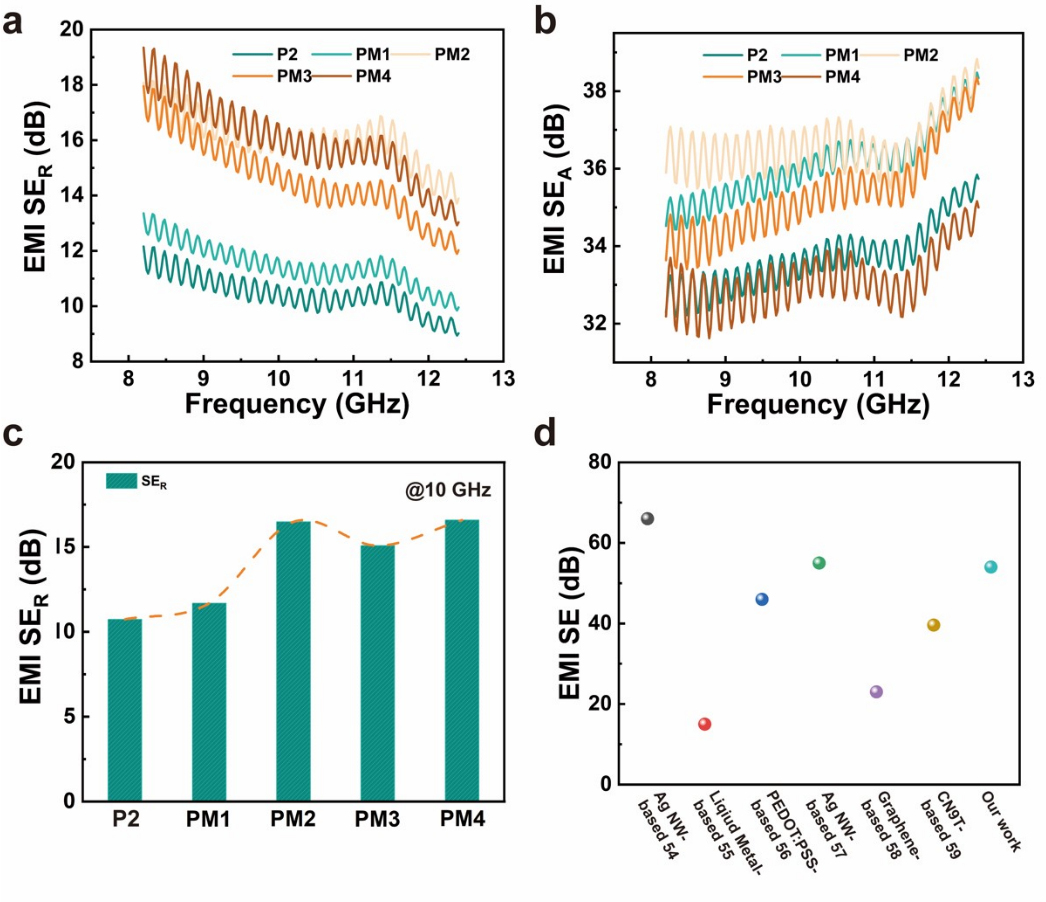

Figure S4. (a) EMI SE$_R$ and (b) EMI SE$_A$ of SCCFs with different Mxene content at 8.2 to 12.4 Hz. (c) EMI SE$_R$ of SCCF with different Mxene content at 10GHz. (d) Comparison of EMI and other flexible conductive composites for wearable electronics.

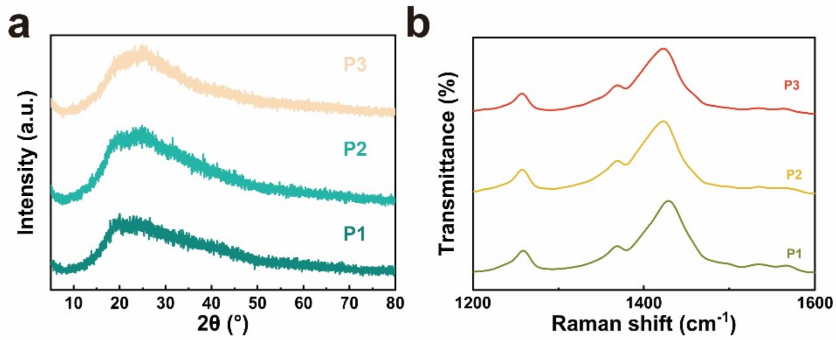

Figure S5. (a) XRD patterns and (b) Raman spectra of the SCCF with different content of PEDOT:PSS.

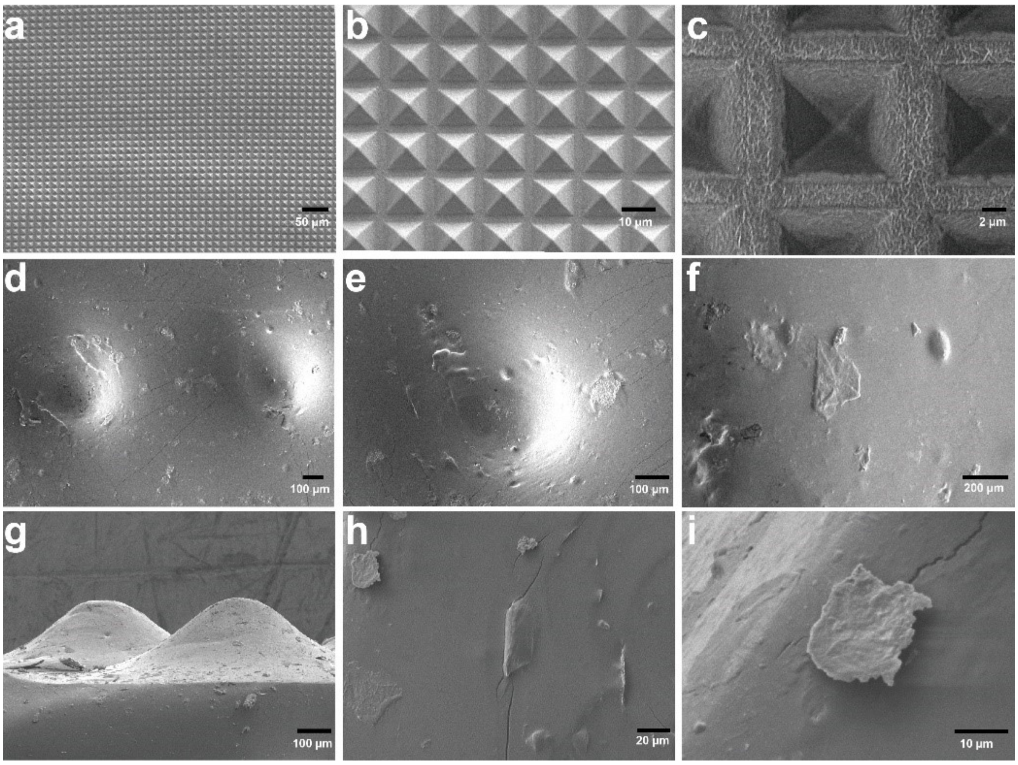

Figure S6. SEM image of (a-c) the pyramid structure of the dielectric layer and (d-f) the SCCFs electrode (PM2) at different magnifications. (g-i) The cross-section image of SCCFs electrode (PM2) at different magnifications.

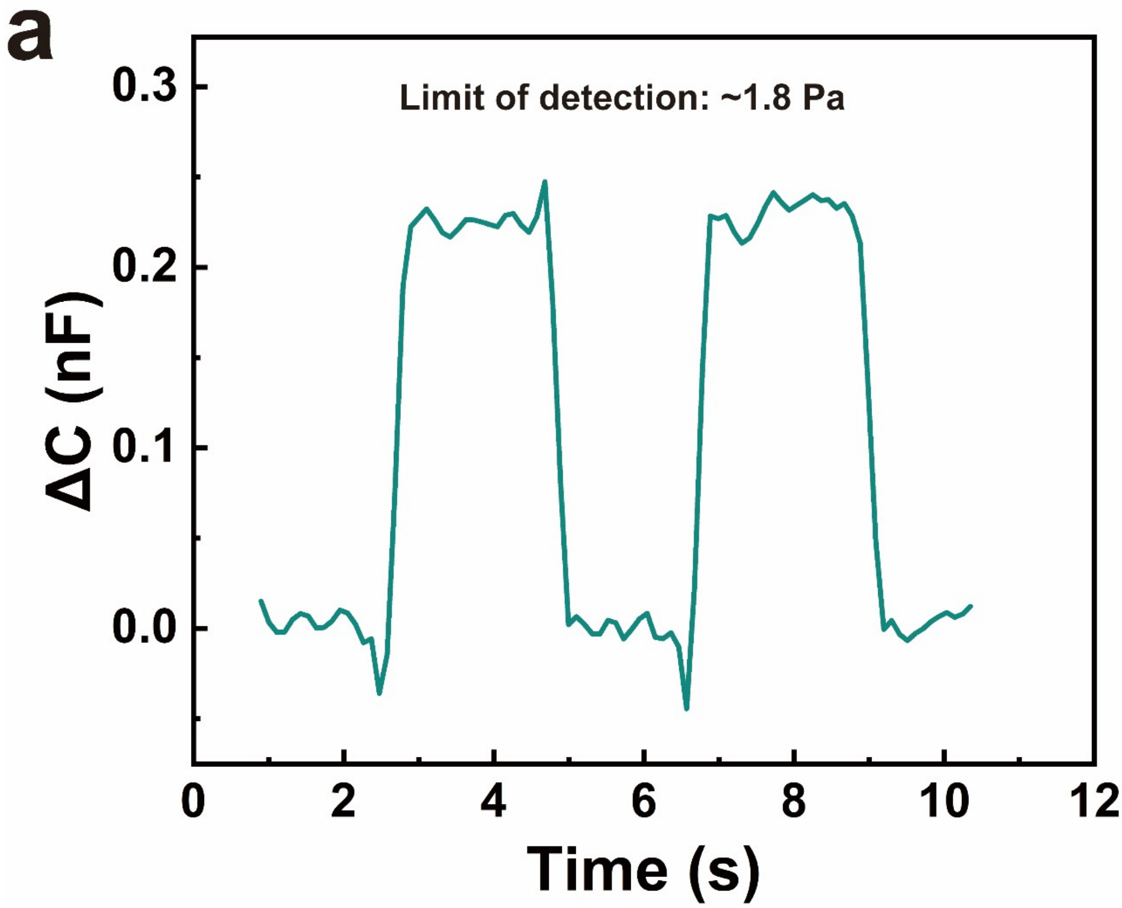

Figure S7. (a) Limitation of detection (LOD) of ~1.8 Pa of the SCCF-based sensor.

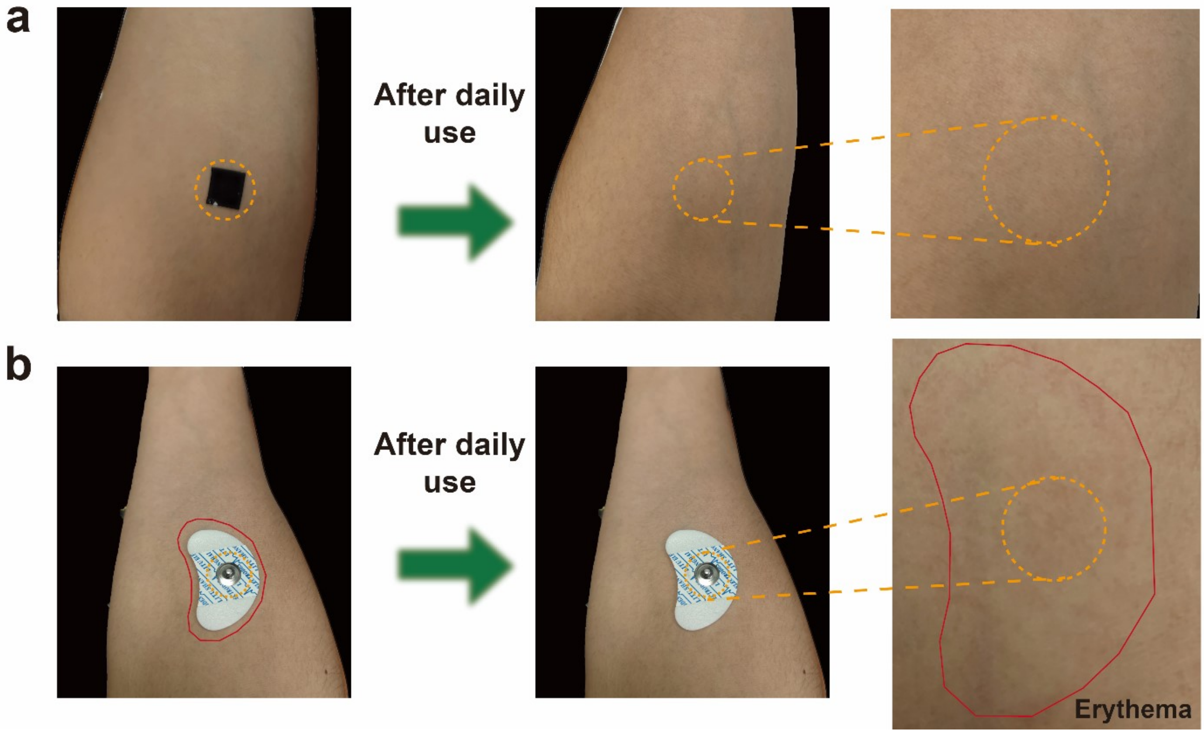

Figure S8. Images of a SCCF attached to the forearm. (a) It has no significant inflammation after one day. (b) After 1 hour of wearing the commercial gel electrodes, the skin has obvious erythema.

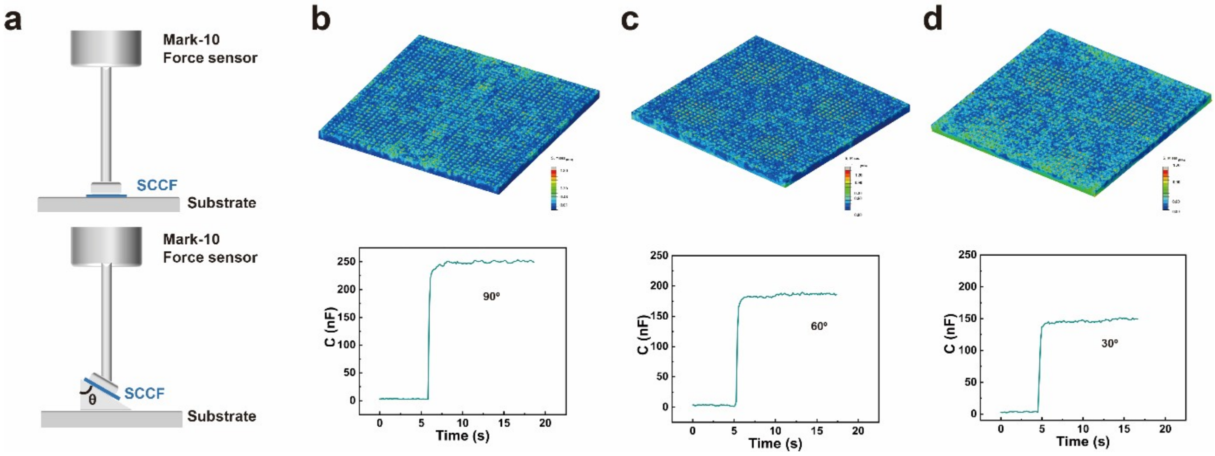

Figure S9. Multidirectional force detection of the SSCF-based sensor. (a) Schematic of the multifunctional force measurement. The simulated stress distribution of the pyramid structure dielectric layer and measured capacitance under (b) 90^{o}, (c) 60^{o}, and (d) 30^{o}.

Table S1 The details of various SCCFs with different PEDOT:PSS and MXene mass ratios.

Sample	SMDES			Polymer solution		PH1000 (1.3wt%)/g	MXene/mg
	β-CD/g	citric acid/g	H_2O/g	10% PVA/g	25% GA/μL		
P1	0.59	1	5	2	5	6	0
P2	0.59	1	5	2	5	13	0
P3	0.295	0.5	2.5	1	2.5	13	0
PM1	0.59	1	5	2	5	13	12
PM2	0.59	1	5	2	5	13	34
PM3	0.59	1	5	2	5	13	85
PM4	0.59	1	5	2	5	13	118